Phytochemistry 106 (2014) 37–43

Contents lists available at ScienceDirect

Phytochemistry

journal homepage: www.elsevier.com/locate/phytochem

Investigation of a substrate-specifying residue within *Papaver somniferum* and *Catharanthus roseus* aromatic amino acid decarboxylases

Michael P. Torrens-Spence, Michael Lazear, Renee von Guggenberg, Haizhen Ding, Jianyong Li *

Department of Biochemistry, Virginia Tech, Blacksburg, VA, United States

ARTICLE INFO

Article history:
Received 10 March 2014
Received in revised form 2 June 2014
Available online 5 August 2014

Keywords:
Papaver somniferum
Papaveraceae
Catharanthus roseus
Apocynaceae
Aromatic amino acid decarboxylase
Tyrosine decarboxylases
Tryptophan decarboxylases

ABSTRACT

Plant aromatic amino acid decarboxylases (AAADs) catalyze the decarboxylation of aromatic amino acids with either benzene or indole rings. Because the substrate selectivity of AAADs is intimately related to their physiological functions, primary sequence data and their differentiation could provide significant physiological insights. However, due to general high sequence identity, plant AAAD substrate specificities have been difficult to identify through primary sequence comparison. In this study, bioinformatic approaches were utilized to identify several active site residues within plant AAAD enzymes that may impact substrate specificity. Next a *Papaver somniferum* tyrosine decarboxylase (TyDC) was selected as a model to verify our putative substrate-dictating residues through mutation. Results indicated that mutagenesis of serine 372 to glycine enables the *P. somniferum* TyDC to use 5-hydroxytryptophan as a substrate, and reduces the enzyme activity toward 3,4-dihydroxy-L-phenylalanine (dopa). Additionally, the reverse mutation in a *Catharanthus roseus* tryptophan decarboxylase (TDC) enables the mutant enzyme to utilize tyrosine and dopa as substrates with a reduced affinity toward tryptophan. Molecular modeling and molecular docking of the *P. somniferum* TyDC and the *C. roseus* TDC enzymes provided a structural basis to explain alterations in substrate specificity. Identification of an active site residue that impacts substrate selectivity produces a primary sequence identifier that may help differentiate the indolic and phenolic substrate specificities of individual plant AAADs.

1. Introduction

Aromatic amino acid decarboxylases (AAADs) are a group of economically important and phylogenetically diverse enzymes that are categorically lined through their pyridoxal 5-phosphate (PLP) dependence and sequence homology. This family of enzymes has been studied extensively in mammals where a single enzyme, 3,4-dihydroxy-L-phenylalanine (dopa) decarboxylase (DDC), catalyzes decarboxylation of both phenolic and indolic amino acids to generate their corresponding aromatic amines. Mammalian DDC is responsible for the decarboxylation of dopa and 5-hydroxytryptophan to yield the neurotransmitters dopamine and serotonin, respectively (Srinivasan and Awapara, 1978; Zhu and Juorio, 1995). Unlike the single mammalian DDC enzyme, plant AAADs have evolved with variations in activity and substrate specificity. The resulting paralogs are formally identified as tryptophan decarboxylases (TDCs), tyrosine decarboxylases (TyDCs) and aromatic acetaldehyde synthases (AASs), respectively. TDCs catalyze decarboxylation of tryptophan and 5-hydroxytryptophan (Noé et al., 1984; De Luca et al., 1988; Lopez-Meyer and Nessler, 1997; Yamazaki et al., 2003; Kang et al., 2007; Park et al., 2009), whereas TyDCs engender decarboxylation of tyrosine and dopa (Facchini and De Luca, 1995; Lehmann and Pollmann, 2009; Torrens-Spence et al., 2012, 2013) and AASs the decarboxylation-oxidative deamination of dopa, tyrosine and phenylalanine (Kaminaga et al., 2006; Gutensohn et al., 2011; Torrens-Spence et al., 2012), respectively.

Differences in substrate selectivity and activity among plant TyDCs, TDCs and AASs enable individual enzymes to generate specific products with unique physiological functions. For example, plant TDCs are required for synthesis of monoterpenoid indole alkaloids that comprise a diverse group of hundreds of pharmacologically active compounds (Meijer et al., 1993; Berlin et al., 1994; Facchini et al., 2000), TyDCs are known to function in several different metabolic pathways including the biosynthesis of simple alkaloids, complex benzylisoquinoline alkaloids, and *N*-hydroxycinnamic acid amides (Leete and Marion, 1953; Ellis,

* Corresponding author. Address: Department of Biochemistry, Engel Hall 204, Virginia Tech, Blacksburg, VA 24061, United States. Tel.: +1 540 321 5779; fax: +1 540 231 9070.
E-mail address: lij@vt.edu (J. Li).

http://dx.doi.org/10.1016/j.phytochem.2014.07.007
0031-9422/

1983; Marques and Brodelius, 1988; Trezzini et al., 1993; Facchini et al., 2000) and AAS enzymes catalyze the production of volatile flower scents, floral attractants, and defensive phenolic acetaldehyde secondary metabolites (Kaminaga et al., 2006; Gutensohn et al., 2011; Torrens-Spence et al., 2012). It is clear that the physiological functions of plant AAADs are closely related to their respective activities and substrate specificities; however, due to the subtlety of the enzymatic divergence of plant AAADs, it has historically been difficult to predict the function of any given plant AAAD paralog through sequence comparison. Consequently, being able to distinguish the activity and substrate specificity of individual plant AAADs is of practical significance.

In previous work, it was determined that a single active site residue is capable of dictating the activity of plant TyDCs, TDCs and AASs without altering substrate selectivity. Specifically, the presence of a tyrosine in an active site catalytic loop dictates decarboxylation chemistry while a phenylalanine substitution at the same location dictates aldehyde synthase chemistry (Torrens-Spence et al., 2013). The alteration in enzymatic activity due to a single amino acid substitution suggests that the functional variations in plant AAADs may be dictated by a small number of residues. Such subtle variations in plant AAADs likely explain the difficulty in differentiating plant TyDCs, TDCs and AASs through sequences analysis.

In this study, to further distinguish plant AAADs an attempt to identify specific structural identifiers capable of differentiating between the substrate specificity of TDCs and TyDCs was made. To do so, bioinformatic analyses of characterized plant AAAD enzymes were performed with predicted several target residues that might potentially impact substrate specificity in plant AAADs and these residues assessed through site-directed mutations using a *Papaver somniferum* TyDC and a *Catharanthus roseus* TDC. Results of the biochemical analyses, in conjunction with molecular modeling, provide insights into a residue that impacts plant AAAD indole and benzene substrate selectivity.

2. Results

2.1. Primary sequence investigation of recombinant characterized TyDC and TDC sequences

To begin the investigation of residues that might impact substrate specificity of plant AAAD enzymes, a primary sequence evaluation of essentially all the characterized plant TyDC and TDC sequences was performed (Supplemental Table S1). Pairwise alignments of these characterized plant AAAD enzymes indicated that inter TDC–TyDC class identities are often greater than that of intra TDC or TyDC classes. For example, despite differences in substrate specificity, the *Capsicum annuum* TDC 2 (Park et al., 2009) shares greater homology with the *Arabidopsis thaliana* TyDC (Lehmann and Pollmann, 2009) (66% identity) than it does with the *Camptotheca acuminata* TDC 2 (Lopez-Meyer and Nessler, 1997) (56% identity). The sequence ambiguity of plant AAADs can be further illustrated in a dendrogram of characterized TyDC and TDC sequences (Fig 1). As this figure illustrates, TyDC and TDC sequences did not appear to exclusively cluster according to their substrate preference. Despite maintaining identical substrate profiles, the characterized TDC sequences appeared to cluster into two groups. Interestingly, TDC sequences from both *Oryza sativa* and *C. annuum* appear in both clusters. This suggests that this clustering is not due to evolutionary divergence of plant species but rather the evolutionary divergence of individual AAAD sequences. In addition to the delocalization of the TDC genes, the dendrogram suggest variable clustering of characterized TyDC sequences. *P. somniferum* TyDC 7, *P. somniferum* TyDC 9 and *Thalictrum flavum* TyDC cluster together while *A. thaliana* TyDC clusters with *O. sativa* TDC 2 and *C. annuum* TDC 2. The sequence and phylogenetic ambiguity of TyDC and TDC enzymes produces significant challenges in plant AAAD gene annotation.

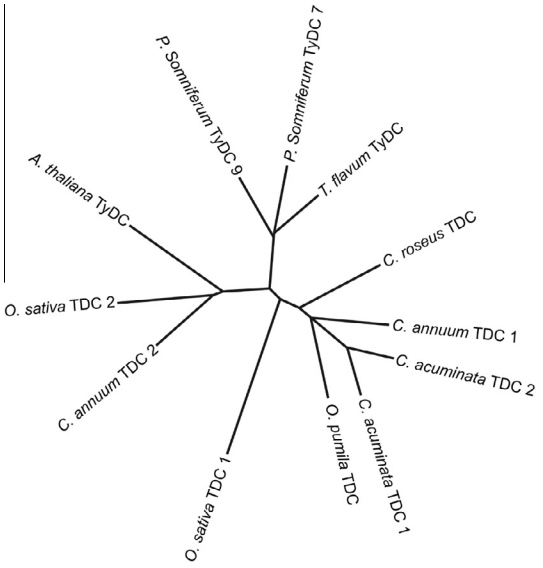

Fig. 1. Dendrogram of recombinantly characterized plant TyDC and TDC sequences.

Multiple sequence alignments of characterized TyDC and TDC sequences were used to identify possible substrate specifying residues. Analysis of residues conserved within 9 or more of the 12 characterized TDC and TyDC sequences yielded twenty-two putative substrate-specifying residues. These conserved residues were highlighted in the *P. somniferum* TyDC 9 sequence (subsequently referred to as *P. somniferum* TyDC) (Torrens-Spence et al., 2013) (Fig. 2). Next, the previously characterized *P. somniferum* TyDC was modeled and a carbidopa external aldimine superimposed into the active site. Residues within four angstroms of the carbidopa external aldimine were highlighted to produce an additional 18 residues potentially involved in substrate recognition (Fig. 2). Cross-referencing these active site proximal residues with the conserved TyDC/TDC residues reduced the hypothetical substrate specifying residues down to 5 individual amino acids (Fig. 2). These residues are represented as serine 101, cysteine 170, asparagine 318, alanine 319 and serine 372 within the *P. somniferum* TyDC sequence.

2.2. Generation and investigation of putative substrate specifying P. somniferum TyDC mutants

Before evaluating the substrate specifying roles of these select five residues, recombinant *P. somniferum* TyDC was first evaluated to determine the substrate range of the wild type TyDC. The recombinant wild type TyDC was expressed and purified to homogeneity. Activity assay results showed that it efficiently catalyzed the decarboxylation of dopa and tyrosine (at 2 mM substrate concentration, the enzyme showed 5910 ± 200 nmol/min/mg protein to dopa and 5350 ± 200 nmol/min/mg protein to tyrosine), but displayed no activity towards phenylalanine or indolic substrates, including 5-hydroxytryptophan and tryptophan. Next, using the *P. somniferum* TyDC as a model, site directed mutations of S101A, C170A, N318S, A319P and S372G were made based on conserved active site proximal residues.

To test perturbations in substrate specificity, the *P. somniferum* TyDC S101A, C170S, N318S, A319P, and S372G mutant enzymes were cloned, expressed, and purified to homogeneity. The activities of the mutant enzymes were tested using dopa, tyrosine,

```
1   MGSLPTNNLE SISLCSQNPL DPDEFRRQGH MIIDFLADYY KNVENYPVRS QVEPGYLKKR
61  LPESAPYNPE SIETILEDVT NDIIPGLTHW QSPNYFAYFP SSGSIAGFLG EMLSTGFNVV
121 GFNWMSSPAA TELESIVMNW LGQMLTLPKS FLFSSDGSSG GGGVLQGTTC EAILCTLTAA
181 RDKMLNKIGR ENINKLVVYA SNQTHCALQK AAQIAGINPK NVRAIKTSKA TNFGLSPNSL
241 QSAILADIES GLVPLFLCAT VGTTSSTAVD PIGPLCAVAK LYGIWVHIDA AYAGSACICP
301 EFRHFIDGVE DADSFSLNAH KWFFTTLDCC CLWVKDSDSL VKALSTSAEY LKNKATESKQ
361 VIDYKDWQIA LSRRFRSMKL WLVLRSYGVA NLRTFLRSHV KMAKHFQGLM GMDNRFEIVV
421 PRTFAMVCFR LKPAAIFKQK IVDNDYIEDQ TNEVNAKLLE SVNASGKIYM THAVVGGVYM
481 IRFAVGATLT EERHVTGAWK VVQEHTDAIL GA
```

Fig. 2. Putative substrate specifying residues form *P. Somniferum* TyDC 9. Green residues are mostly conserved (residues are conserved between substrate specificities for 8 or more of the 11 characterized TDC and TyDC sequences). Red residues are within 4 Å of the carbidopa external aldimine from the TyDC 9 homology model. Yellow residues are amino acids that appear as both green and red residues. Residues in bold and italic indicate amino acids within 4 Å of the carbidopa external aldimine from the beta chain of the homodimer. (For interpretation of the references to color in this figure legend, the reader is referred to the web version of this article.)

phenylalanine, tryptophan and 5-hydroxytryptophan. Results indicated that the S101A, C170S, N318S and A319P mutants had no obvious alterations in indolic or phenolic substrate specificity. However, the S372G mutant displayed a broader substrate profile. The S372G mutant retained activity towards dopa and tyrosine, had no measurable activity towards tryptophan (Supplementary Fig. 1A–D), but displayed activity towards 5-hydroxytryptophan (Fig 3A–D). Initial biochemical testing suggested that the *P. somniferum* TyDC serine 372 residue might play a role in differentiating phenolic substrates from indolic substrates. To measure alterations in substrate selectivity, a full kinetic characterization of the S372G and wild type *P. somniferum* TyDC enzymes was performed using the preferred substrate (dopa) and the putative indolic substrate (5-hydroxytryptophan). The calculated kinetic parameters indicated that the mutation reduced the enzyme's ability to catalyze decarboxylation of dopa, while enabling a new but weak 5-hydroxytryptophan decarboxylase activity (Table 1). No kinetic data for 5-hydroxytryptophan was obtainable for the wild type TyDC due to the lack of measurable product formation. Comparative sequence analysis of residues homologous to the *P. somniferum* TyDC 372 residue revealed that serine was stringently conserved in all experimentally verified TyDC

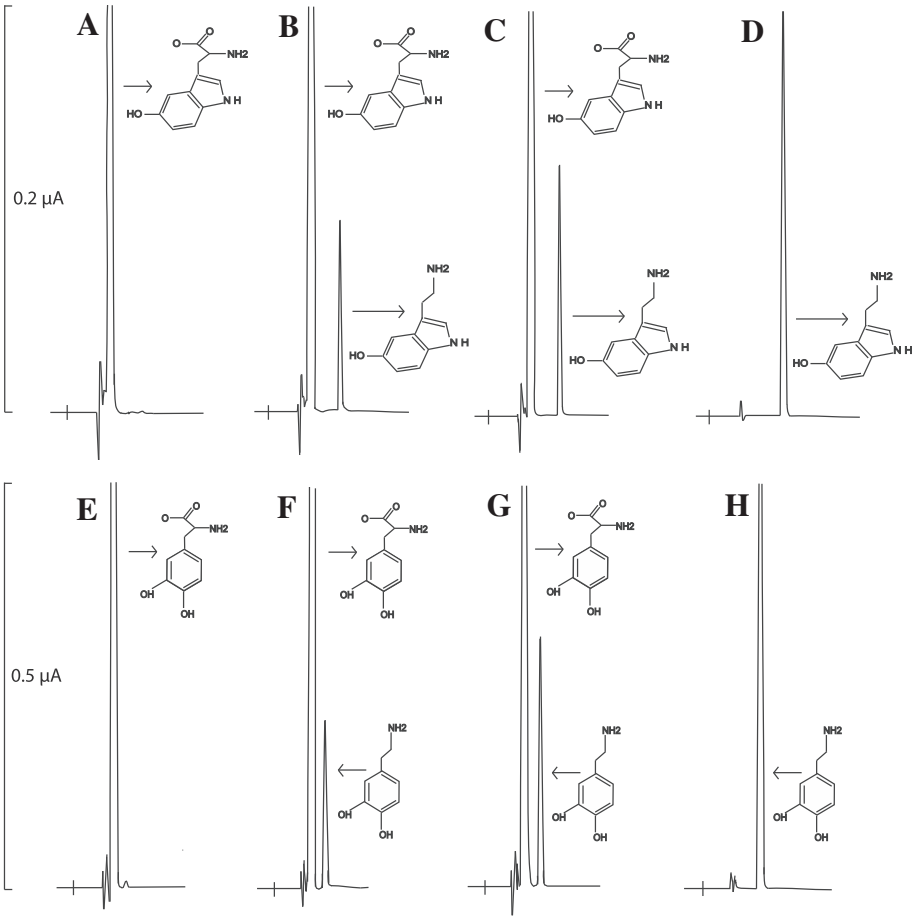

Fig. 3. HPLC-EC detection of products from *P. somniferum* TYDC S372G and *C. roseus* TDC G370S mutants. The *Y*-axis represents the output in microamps, the *x*-axis represents retention time. Chromatogram (A) illustrates lack of product formed from *P. somniferum* TyDC wild type and 5-hydroxytryptophan after 20 min of incubation. Chromatograms (B) illustrate the formation of 5-hydroxytryptamine generated from 5-hydroxytryptophan and the *P. somniferum* TyDC S372G mutant after 10 min of incubation. Chromatograms (C) illustrate the formation of 5-hydroxytryptamine generated from 5-hydroxytryptophan and the *P. somniferum* TyDC S372G after 20 min of incubation. Chromatogram (D) shows the peak generated from the injection of 150 pmol of 5-hydroxytryptamine standard. Chromatogram (E) illustrates the lack of product formed from the *C. roseus* TDC wild type and the dopa reaction mixture after 20 min of incubation. Chromatogram (F) illustrate the formation of dopamine generated from incubating dopa and the *C. roseus* TDC G370S mutant for 10 min. Chromatograms (G) illustrate the formation of dopamine generated from dopa and the *C. roseus* TDC G370S mutant after 20 min of incubation. Chromatogram (H) shows the peak generated from the injection of 150 pmol of dopamine standard.

Table 1
Kinetic parameters of Papaver somniferum wild type and mutant TyDC9 enzymes.

Substrate	Enzyme	kcat (1/s)	Error (1/s)	K_m (mM)	Error (mM)	kcat/K_m (1/(s mM))	Error (1/(s mM))
Dopa	PsTyDC (WT)	8.02	0.46	0.75	0.10	10.97	0.66
Dopa	PsTyDC (S372G)	1.47	0.30	2.10	0.20	0.72	0.21
5-Hydroxytryptophan	PsTyDC (WT)	ND	ND	ND	ND	ND	ND
5-Hydroxytryptophan	PsTyDC (S372G)	0.26	0.03	3.95	0.45	0.07	0.01
Tryptophan	CrTDC (WT)	2.54	0.10	0.12	0.02	21.92	4.49
Tryptophan	CrTDC (G370S)	1.37	0.11	0.21	0.05	7.05	2.20
Dopa	CrTDC (WT)	ND	ND	ND	ND	ND	ND
Dopa	CrTDC (G370S)	0.37	0.04	3.40	0.21	0.11	0.01

Values represent mean SE ($n = 3$).
ND, not determined.

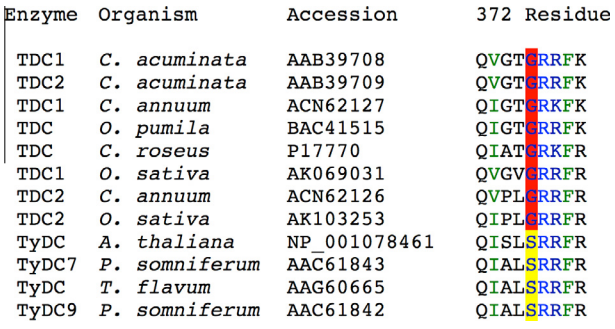

Fig. 4. Sequence alignment of a key residue within the characterized TDC and TyDC sequences. Within the TDC sequences, the residue homologous to the *P. somniferum* TYDC serine 372 is highlighted in red. Within the TyDC sequences, the residue homologous to the *P. somniferum* TYDC serine 372 is highlighted in yellow. (For interpretation of the references to color in this figure legend, the reader is referred to the web version of this article.)

enzymes, while glycine was conserved in all experimentally verified TDC enzymes (Fig 4).

2.3. Generation and biochemical investigation of the C. roseus G 370S TDC mutant

Based on the findings from the mutation of the S372 TyDC residue, a similar study was conducted to broaden the substrate specificity of a TDC to include phenolic substrates. A *C. roseus* TDC was selected as the candidate for this study and a TDC G370S mutant was expressed, purified and evaluated for altered substrate specificity. This TDC, like other verified TDCs, contains the conserved glycine 370 (equivalent to serine 372 of the *P. somniferum* TyDC) (Fig 4). An electrochemical HPLC assay determined that, unlike the wild type enzyme, the *C. roseus* TDC G370S mutant was able to catalyze decarboxylation of dopa (Fig 3E–H) and tyrosine (Supplementary Fig. 2A–D). The *C. roseus* TDC G370S enzyme displayed no activity towards phenylalanine (Supplementary Fig. 1E–G). Full kinetic characterization of the G370S and wild type *C. roseus* TDCs showed significant alterations in the enzyme's substrate profile. Comparison of the kinetic values between the wild type TDC and the mutant TDC illustrated that the glycine 370 serine substitution reduces binding affinity and the rate of the enzyme towards tryptophan while enabling the enzyme to utilize dopa as a substrate (Table 1).

2.4. Molecular modeling of the substrate-impacting residue

Homology models of *P. somniferum* TyDC wild type, *P. somniferum* TyDC S372G, *C. roseus* TDC wild type and *C. roseus* TDC G370S were generated and analyzed in an effort to investigate the structure–function relationship of the specificity-impacting residue. To reveal the possible interactions of the enzyme with its substrates, a carbidopa external aldimine was superimposed into the active site of the models. Model analysis suggests likely involvement of the serine 372 (TyDC sequence) and glycine 370 (TDC sequence) in substrate recognition. In the ligand bound models, this residue was located in the back of the active site approximately three to five angstroms away from the 3′ hydroxyl of the carbidopa external aldimine (Fig 5). Comparison of the wild type and mutant models indicated that the mutations altered the size of the active site pocket by approximately one and a half angstroms. For example, within the *P. somniferum* TyDC model, the serine 372 glycine mutation increases the distance between the 3 prime hydroxyl group of the carbidopa ligand and the 372 residue from 3.6 Å to 5.0 Å. Conversely, the reverse mutation in the *C. roseus* TDC enzyme decreases the distance from 5.0 Å to 3.6 Å. The theoretical alterations in active site volume might enable the accommodation of specific sizes of substrates, whereas the structurally larger serine residue may reduce the size of the active site to accommodate phenolic substrates while the structurally smaller glycine residue may increase the size of the active site to accommodate larger indolic compounds. Biochemical characterization of the substrate-impacting residue, in coordination with the ligand bound homology model analyses, helps to illuminate the functional roles of these active site residues.

3. Discussion

Previous work identified a single residue responsible for differentiation of AAAD and AAS activity. Within plant AAADs and AASs, the presence of the active site tyrosine residue appears to dictate

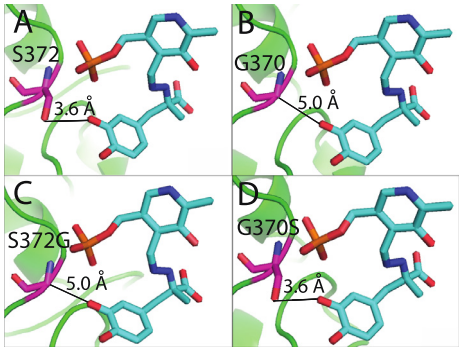

Fig. 5. Homology model active site analysis of the *P. somniferum* TyDC wild type, the *P. somniferum* TyDC S372G, the *C. roseus* TDC wild type and the *C. roseus* TDC G370S mutant. Ligands and models were generated using the PDB model 1JS3. The blue structure represents the external aldimine of carbidopa and PLP. The magenta residue represents the substrate impacting amino acid. Model (A) illustrates the distance between the ligand and *P. somniferum* TyDC wild type 372 residue. Model (B) illustrates the distance between the ligand and *C. roseus* TDC wild type 370 residue. Model (C) illustrates the distance between the ligand and *P. somniferum* TyDC mutant residue 372. Model (D) illustrates the distance between the ligand and *C. roseus* TDC mutant residue 370. (For interpretation of the references to color in this figure legend, the reader is referred to the web version of this article.)

decarboxylation activity, while a phenylalanine substitution seems tobe responsible for decarboxylation-oxidative deamination activity (Torrens-Spence et al., 2013). The resulting research indicates that biochemical and biophysical characteristics of individual active site amino acids may promote/enhance specific catalytic reactions; thereby dictating their reaction chemistry. Consequently, it is reasonable to suggest that the molecular mechanism responsible for differentiating plant AAADs may be dictated by a select few amino acids.

TDCs and TyDCs have different physiological functions; therefore being able to distinguish substrate selectivity without lab-intensive experimental verification is highly useful. Despite their high sequence identity, it is well known that plant TyDCs do not use indolic amino acids as substrate and TDCs have no any activity to amino acids with benzene rings. The rigorous substrate selectivity of both TDCs and TyDCs has been stressed in many publications (De Luca et al., 1988; Facchini and De Luca, 1995; Facchini et al., 2000). Moreover, sequence analysis and hydropathy plots suggest that the unique substrate specificity of plant TyDCs and TDCs are the result of relatively minor amino acid substitutions (De Luca et al., 1988; Facchini and De Luca, 1995; Facchini et al., 2000).

In this study, attempts were made to identify key residues capable of differentiating the phenolic selective TyDCs from indolic selective TDCs. Extensive comparative analyses of characterized TyDC and TDC sequences enabled us to select several potential target residues. Site-directed mutagenesis of these residues within two model enzymes provided evidence to suggest that the *P. somniferum* TyDC 372 residue and the *C. roseus* TDC 370 residue collectively impact substrate selectivity. The new found activity of the *P. somniferium* S372G TyDC towards 5-hydroxytryptophan and the *C. roseus* G370S TDC towards dopa appears to be significant. The kinetic values of these mutant enzymes and their new substrates are comparable to some characterized AAAD enzymes. For example, the *k*cat values of the two mutant enzymes towards their new substrates are larger than the *k*cat values of *C. annuum* TDC 1 and *C. annuum* TDC 2 [Park et al., 2009] towards their preferred substrate tryptophan. Moreover, the substrate specificity of the mutants towards their new substrates is comparable to those of an investigated orphan TDC enzyme (K_m 3.0 mM towards tryptophan) (Gibson et al., 1972). Although both mutations enabled expanded substrate profiles, the substitutions did not lead to loss of their original activities. However, it is reasonable to suggest that this active site residue is a key amino acid responsible for impacting substrate specificity. This hypothesis is supported by the glycine conservation in verified TDCs and the serine conservation in verified TyDCs (Fig. 4).

Subsequent analysis of the active site conformation of the *C. roseus* TDC and *P. somniferum* TyDC ligand bound homology models provides some structural basis for alterations in substrate profiles. It can be proposed that the mutation of the *P. somniferum* 372 residue from serine to glycine enables broader substrate selectivity by increasing the active site to accommodate structurally large substrates like 5-hydroxytryptophan, while the *C. roseus* G370S mutation reduces the size of the active site to accommodate the structurally smaller dopa. Molecular interaction measurements support this hypothesis. Homology models of the two mutants illustrate an alteration of active site pocket of 1.4 Å. The altered volume of the active site could enable structurally different compounds to enter the active site and form the external aldimine with the PLP cofactor.

A brief Genbank evaluation of this 372 residue AAAD has been performed in an effort to annotate non-characterized plant AAAD sequences using the results from this study. An analysis of the NCBI plants (taxid: 3193) database enables tentative identification of several sequences annotated as TyDCs that are likely TDCs. For example, based on the conservation of the homologous G372 residue (implicating indolic substrate specificity) and the presence of the homologous Y350 residue (implicating decarboxylation activity and not aldehyde synthase activity) (Torrens-Spence et al., 2013), it can be speculated that the annotated *Fragaria vesca* TyDC, *Medicago truncatula* TyDC, *Setaria italica* TyDC and *Theobroma cacao* TyDC sequences are all likely TDCs. Such primary sequence annotation illustrates the practicality of substrate specificity and activity differentiation within plant type II PLP decarboxylases. The study herein is, therefore, one step towards a better classification of plant TyDCs and TDCs.

4. Concluding remarks

The functional evolution of AAAD enzymes within different branches of the phylogenetic tree reflects the physiological needs of different species. In plants, AAADs are an integral part of the pathways for the biosynthesis of numerous chemical compounds responsible for mitigating interactions with their biotic and abiotic environments (Leete and Marion, 1953; Ellis, 1983; Meijer et al., 1993; Trezzini et al., 1993; Berlin et al., 1994; Facchini et al., 2000). For example, *P. somniferum* contains approximately 15 TyDC sequences that play roles in production of benzylisoquinoline alkaloids, such as the pharmacologically active morphine, codeine and papaverine (Facchini and De Luca, 1995; Facchini et al., 2000). However, despite variable functions, plant TyDCs and TDCs do not have easily recognizable motifs in primary sequences. Although it is sometimes possible to classify the substrate specificity of a given AAAD through extensive sequence comparison, plant AAAD differentiation remains quite speculative. The findings regarding the S372G and G370S mutants indicate that the phenolic and indolic substrates in plant AAADs could be primarily dictated by this single active site amino acid. The stringent conservation for serine and glycine in verified plant TyDC and TDC, respectively, support this consideration (Fig 4). Future research is needed to fully reveal the active site conformations and residues invariably conserved amongst distinct plant AAAD classes. Upon completion, AAAD fingerprints should enable the proper annotation of AAAD and AAS genes without expensive and laborious enzyme expression and characterization.

5. Experimental

5.1. Reagents

Tyrosine, tyramine, tryptophan, tryptamine, 5-hydroxytryptophan, 5-hydroxytryptamine, dopa, dopamine, phenylalanine, phenylethylamine, pyridoxal 5-phosphate (PLP), phthaldialdehyde, HCO_2H, and CH_3CN were purchased from Sigma (St. Louis, MO). The IMPACT-CN protein expression system was purchased from New England Biolabs (Ipswich, MA).

5.2. Preparation of recombinant proteins

P. somniferum and *C. roseus* RNA extraction, cDNA production, vector cloning and wild type protein expression were conducted as previously described (Torrens-Spence et al., 2013). Primer pairs were synthesized and used for amplification and SapI mutagenesis of the expression mutants (Supplemental Table S2). The resulting PCR products were ligated together into IMPACT-CN bacterial expression plasmids. DNA sequencing was utilized to verify the sequence and frame of each mutant cDNA insert. Transformed bacterial colonies, expressing the wild type and mutant proteins, were selected and used for large-scale expression of individual recombinant proteins. Bacterial cells were cultured at 37 °C. After induction with 0.15 mM IPTG, the cells were cultured

at 15 °C for 24 h. The soluble fusion proteins were applied to a column packed with chitin beads and subsequently hydrolyzed under reducing conditions. The affinity purification resulted in the isolation of each individual recombinant protein at about 85% purity. Further purifications of recombinant proteins were achieved by Mono-Q and gel filtration chromatography. Purified recombinant enzymes were concentrated to approximately 10 mg/ml protein in 25 mM HEPES (pH 7), containing 0.04 mM PLP using a Centricon YM-50 concentrator (Millipore). Purity of the recombinant proteins was evaluated by SDS–PAGE. The concentrations of the purified recombinant proteins were determined by a Bio-Rad protein assay kit (Hercules, CA) using bovine serum albumin as a standard.

5.3. Homology modeling and ligand superimposition

Modeller (Šali and Blundell, 1993) was utilized to produce ten *P. somniferum* TyDC and *C. roseus* TDC homology models for the substrate analog bound protein data bank models 1JS3 (Burkhard et al., 2001). The model from each PDB template with the optimal molpdf and DOPE score were selected for further evaluation. Mutant homology models were generated in the same manner from the optimal wild type models. Pymol was utilized to align the PLP coenzyme and substrate analog from 1JS3 (Burkhard et al., 2001) onto the corresponding homology models and to visualize the active site residues. The residues proximal to the ligand from the homology models were then compared with their homologous residues from characterized TyDC and TDC enzymes to identify potential substrate specifying residues.

5.4. Kinetic analysis

The specific activity of the wild type *P. somniferum* TyDC towards tyrosine and dopa was analyzed in 50 µl phosphate buffer (pH 7.5) containing 2 mM substrate with enzyme (2 µg) for an incubation time of 2.5 min. This analysis determined that the wild type enzyme possessed typical TyDC activity. The S372G mutant displayed both typical TyDC activity and novel decarboxylation activity towards 5-HTP. The kinetic parameters of the *P. somniferum* TyDC wild type, *P. somniferum* S372G mutant, *C. roseus* TDC wild type and *C. roseus* TDC G370S mutant enzymes were subsequently analyzed. Reaction mixtures of 50 µl assays containing recombinant protein (25 µg for *P. somniferum* TyDC 5-hydroxytryptophan, 3 µg for the *P. somniferum* TyDC dopa, 25 µg for C. *roseus* TDC dopa and 3 µg for the *C. roseus* TDC tryptophan) and varying concentration of substrate (0.05–20 mM of 5-hydroxytryptophan, 0.005–5 mM of tryptophan and 0.05–15 mM of dopa) were prepared in 50 mM phosphate buffer (pH 7.5) and incubated at 25 °C. An equal volume of 0.8 M HCO_2H was added to each reaction mixture (15 min for *P. somniferum* TyDC 5-hydroxytryptophan assays, 2.5 min for *P. somniferum* dopa assays, 15 min for *C. roseus* TDC dopa assays and 2.5 min for *C. roseus* tryptophan assays) with supernatants individually was subjected to HPLC-electrochemical analysis. Kinetic data points were performed in triplicate and kinetic values were evaluated by hyperbolic regression. An isocratic running buffer consisting of 50 mM phosphate buffer pH 4.3, 25% acetonitrile, and 0.5 mM octyl sulfate was used for the 5-hydroxytryptophan characterization, whereas an isocratic running buffer consisting of 50 mM phosphate buffer pH 4.3, 15% acetonitrile, and 0.5 mM octyl sulfate was used for the dopa characterization. The amounts of products in reaction mixtures containing different concentrations of substrate were quantified based on a standard curve generated using authentic standards at identical conditions of HPLC-electrochemical analysis.

6. Bioinformatic analysis sequences

All of the following accession numbers are from the NCBI Genbank

C. acuminata TDC 1 [AAB39708], *C. acuminata* TDC 2 [AAB39709], *C. annuum* TDC 1 [ACN62127], *C. annuum* TDC 2 [ACN62126], *O. pumila* TDC [BAC41515], *O. sativa* TDC 1 [AK069031], *O. sativa* TDC 2 [AK103253], *C. roseus* TDC [P17770], *P. somniferum* TYDC 9 [AAC61842], *P. somniferum* TyDC 7 [AAC61843], *T. flavum* TyDC [AAG60665], and *A. thaliana* TyDC [NP_001078461], *P. crispum* TyDC [Q06086], *S. lycopersicum* AAAD 1A [NP_001233845], *S. lycopersicum* AAAD 1B [NP_001233852], *S. lycopersicum* AAAD 2 [NP_001233859], *P. somniferum* TyDC 1 [P54768], *P. somniferum* TyDC 2 [P54769], *Fragaria vesca* TyDC [XP_004292248], *Medicago truncatula* TyDC [XP_003625397], *Setaria italica* TyDC [XP_004956078] and *Theobroma cacao* TyDC [EOX99271].

Acknowledgement

This study was supported through Virginia Tech Biochemistry College of Agricultural and Life Sciences funding.

Appendix A. Supplementary data

Supplementary data associated with this article can be found, in the online version, at http://dx.doi.org/10.1016/j.phytochem.2014.07.007.

References

Berlin, J., Ruegenhagen, C., Kuzovkina, I.N., Fecker, L.F., Sasse, F., 1994. Are tissue cultures of *Peganum harmala* a useful model system for studying how to manipulate the formation of secondary metabolites? Plant Cell Tissue Organ Cult. 38, 289–297.

Burkhard, P., Dominica, P., Borri-Voltattorni, C., Jansonius, J.N., Malashkevich, V.N., 2001. Structural insight into Parkinson's disease treatment from drug-inhibited DOPA decarboxylase. Nat. Struct. Biol. 8 (11), 963–967.

De Luca, V., Marineau, C., Brisson, N., 1988. Molecular cloning and analysis of cDNA encoding a plant tryptophan decarboxylase: comparison with animal dopa decarboxylase. PNAS 86 (8), 2582–2586.

Ellis, B.E., 1983. Production of hydroxyphenylethanol glycosides in suspension-cultures of *Syringa vulgaris*. Phytochemistry 22, 1941–1943.

Facchini, P.J., De Luca, V., 1995. Expression in *Echerichia coli* and partial characterization of two tyrosine/dopa decarboxylases from opium poppy. Phytochemistry 38, 1119–1126.

Facchini, P.J., Huber-Allanach, K.L., Tari, L.W., 2000. Plant aromatic L-amino acid decarboxylases: evolution, biochemistry, regulation, and metabolic engineering applications. Phytochemistry 54, 121–138.

Gibson, R.A., Barret, G., Wightman, F., 1972. Biosynthesis and metabolism of indol-3yl-acetic acid: III. Partial purification and properties of a tryptamine-forming L-tryptophan decarboxylase from tomato shoots. J. Exp. Bot. 23 (3), 775–789.

Gutensohn, M., Klempien, A., Kaminaga, Y., Nagegowda, D.A., Negre-Zakharov, F., Huh, J.H., Luo, H., Weizbauer, R., Mengiste, T., Tholl, D., Dudareva, N., 2011. Role of aromatic aldehyde synthase in wounding/herbivory response and flower scent production in different Arabidopsis ecotypes. Plant J. 66, 591–602.

Kaminaga, Y., Schnepp, J., Peel, G., Kish, C.M., Ben-Nissan, G., Weiss, D., Orlova, I., Lavie, O., Rhodes, D., Wood, K., Porterfield, D.M., Cooper, A.J., Schloss, J.V., Pichersky, E., Vainstein, A., Dudareva, N., 2006. Plant phenylacetaldehyde synthase is a bifunctional homotetrameric enzyme that catalyzes phenylalanine decarboxylation and oxidation. J. Biol. Chem. 281, 23357–23366.

Kang, S., Kang, K., Lee, K., Back, K., 2007. Characterization of rice tryptophan decarboxylases and their direct involvement in serotonin biosynthesis in transgenic rice. Planta 227, 263–272.

Leete, E., Marion, L., 1953. The biogenesis of alkaloids: VI. The formation of hordenine and N-methyltyramine from tyrosine in barley. Can. J. Chem. 31, 126–128.

Lehmann, T., Pollmann, T., 2009. Gene expression and characterization of a stress-induced tyrosine decarboxylase from *Arabidopsis thaliana*. FEBS Lett. 583, 1895–1900.

Lopez-Meyer, M., Nessler, C.L., 1997. Tryptophan decarboxylase is encoded by two autonomously regulated genes in *Camptotheca acuminata* which are differentially expressed during development and stress. Plant J. 11, 1167–1175.

Marques, I.A., Brodelius, P.E., 1988. Elicitor-induced L-tyrosine decarboxylase from plant cell suspension cultures. Plant Physiol. 88, 46–51.

Meijer, A.H., Verpoorte, R., Hoge, J.H.C., 1993. Regulation of enzymes and genes involved in terpenoid indole alkaloid biosynthesis in *Catharanthus roseus*. J. Plant Res. 3, 145–164.

Noé, W., Mollenschott, C., Berlin, J., 1984. Tryptophan decarboxylase from *Catharanthus roseus* cell suspension cultures: purification, molecular and kinetic data of the homogenous protein. Plant Mol. Biol. 3 (5), 281–288.

Park, S., Kang, K., Lee, K., Choi, D., Kim, Y., Back, K., 2009. Induction of serotonin biosynthesis is uncoupled from the coordinated induction of tryptophan biosynthesis in pepper fruits (*Capsicum annuum*) upon pathogen infection. Planta 230, 1197–1206.

Šali, A., Blundell, T.L., 1993. Comparative protein modelling by satisfaction of spatial restraints. J. Mol. Biol. 234, 779–815.

Srinivasan, K., Awapara, J., 1978. Substrate specificity and other properties of DOPA decarboxylases from guinea pig kidneys. BBA Enzymol. 526, 597–604.

Torrens-Spence, M.P., Gillaspy, G., Zhao, B., Harich, K., White, R.H., Li, J., 2012. Biochemical evaluation of a parsley tyrosine decarboxylase results in a novel 4-hydroxyphenylacetaldehyde synthase enzyme. Biochem. Biophys. Res. Commun. 2, 211–216.

Torrens-Spence, M.P., Liu, P., Ding, H., Harich, K., Gillaspy, G., Li, J., 2013. Biochemical evaluation of the decarboxylation and decarboxylation-deamination activities of plant aromatic amino acid decarboxylases. J. Biol. Chem. 288, 2376–2387.

Trezzini, G.F., Horrichs, A., Somssich, I.E., 1993. Isolation of putative defense-related genes from *Arabidopsis thaliana* and expression in fungal elicitor-treated cells. Plant Mol. Biol. 21, 385–389.

Yamazaki, Y., Sudo, H., Yamazaki, M., Aimi, N., Saito, K., 2003. Camptothecin biosynthetic genes in hairy roots of *Ophiorrhiza pumila*: cloning, characterization and differential expression in tissues and by stress compounds. Plant Cell Physiol. 44, 395–403.

Zhu, M.-Y., Juorio, A.V., 1995. Aromatic L-amino acid decarboxylase: biological characterization and functional role. Gen. Pharmacol.: Vasc. Syst. 26, 681–696.